Supporting Information

Filteau et al. 10.1073/pnas.1409938112

SI Methods

Candidate PKA Regulator Identification. PKA assays and strain manipulations were performed in four replicates using robotically manipulated 96-, 384-, and 1,536-pin tools (pin length, 38.1 mm; pin diameter 0.787 mm, 0.457 mm, and 0.457 mm, respectively) (V&P Scientific). We introduced the DHFR-fusion PKA subunits into homozygous deletion backgrounds following the procedure developed by Diss et al. (1) (Fig. S1) using synthetic genetic array (SGA) markers (2). To control for the growth defects associated with gene deletions on methotrexate that would be independent of the DHFR PCA signal, we measured the interaction between two exogenous leucine-zipper (ZL) moieties fused to each DHFR fragment in each of the deletion backgrounds, p41-ZL-DHFR[1,2] and p41-ZL-DHFR[3] (3). These plasmids were transformed respectively into BY4741 and BY4742 (strains GD005 and GD006), which went through the same SGA process as the DHFR-fusion PKA subunits. These ZL–ZL control strains and the PKA reporter arrays were organized the same way on the 1,536 high-density arrays, thus allowing mutant fitness reduction to correct for mutant fitness on methotrexate and positional bias at the same time.

Images were analyzed using custom scripts written in ImageJ 1.45s (National Institutes of Health). Raw interaction scores were estimated by measuring colony sizes as described by Diss et al. (1). Colony sizes at days two and four were used to compute PKA interaction scores. Values were first $\log_2$ transformed and adjusted for plate bias by subtracting plate mean values. The difference between each adjusted growth value and the corresponding ZL–ZL control replicate mean was calculated. The PKA interaction score is the average of these differences (four replicates at two time points). Positions with more than two missing data points out of eight for either the PKA assay or the ZL–ZL controls were discarded. PKA interaction scores were averaged when deletion strains were present at multiple positions (14 strains). A confidence value on the PKA interaction score was computed by performing Welch's test comparing growth between PKA and ZL–ZL control colonies and computing an FDR-corrected *P* value. PKA interaction scores were distributed randomly across the four arrays composing the assay, indicating no remaining bias in plate position. Assay plates included 617 positions filled with the *ho*Δ strain as an empirical false-positive control, a wild-type–like strain because the *HO* gene is inactivated in all strains of the BY background. By the FDR of Welch's test at a threshold <0.05 and a PCA interaction score ≤0.5 or >0.5, an average of 5% of *ho*Δ control positions were false positive in each assay (Fig. S2).

Confirmation of Candidates by Spot Dilution Assay and High-Resolution Growth Monitoring in Liquid Cultures. Confirmation strains were reconstructed manually by PCR-mediated gene deletion. First, two strains were constructed by fusing either *TPK1* or *TPK2* with the DHFR F[1,2] fragment in a *BCY1*-DHFR F[3] strain from the *MAT*α PCA collection, using oligonucleotides *TPK1*-DHFR_F/*TPK1*-DHFR_R and *TPK2*-DHFR_F/*TPK2*-DHFR_R and template plasmid pAG25-linker-F[1,2]-ADHterm. Selection on yeast extract/peptone/dextrose (YPD) + Hygromycin B (HygB) + nourseothricin led to strains JFL003 and JFL004, respectively. Confirmation of the gene fusion was obtained by colony PCR. For each candidate, the KANMX or URA3 deletion cassette was amplified by PCR from the pUG6 or pUG72 plasmid, respectively, and was transformed in each of the two strains; the correct gene deletions were verified by colony PCR. These strains were then mated with the corresponding deletion strains from the Yeast Knock-Out collection (4) or the *MAT**a*** SGAready collection (1). As controls, plasmids expressing a leucine zipper moiety fused to either DHFR F[1,2] (p41-ZL-DHFR[1,2]) or DHFR F[3] (p41-ZL-DHFR[3]) (3) were transformed into deletion strains from the Yeast Knock-Out collection (4) or the *MAT*α SGAready deletion collection (1), respectively. Strains with the same deletion but expressing ZL fused to complementary DHFR fragments were mated, and diploid cells were selected on YPD + G418 + nourseothricin + HygB. One colony of each diploid selection was grown overnight at 30 °C in 400 μL of the corresponding diploid-selection medium. Five microliters of each preculture were then used to inoculate 400 μL of synthetic complete (SC)/PCA medium and were grown overnight at 30 °C. Each culture was adjusted to an OD_{600}/mL of 1 and was diluted five times with a dilution factor of 5. Four microliters of each dilution were then spotted on each medium. In addition, high-resolution growth profiling was performed for some strains using qPCA as described by Freschi et al. (5).

Coimmunoprecipitation and Western Blotting. Two candidate regulators of the PKA, *CCZ1* and *SAP30*, were tested by coimmunoprecipitation of the Tpk2–Bcy1 complex. *BCY1* and *TPK2* from the GFP collection (Life Technologies) were used for strain constructions. In the *BCY1*-GFP strain, *TPK2* was fused to the 6HA epitope by PCR-mediated insertion of a cassette amplified from pYM17 (6) using oligonucleotides Tpk2-toolbox_F/Tpk2-toolbox_R, leading to strain AKD228. Correct cassette insertion was verified by colony PCR with oligonucleotides toolbox R and Tpk2_C. Genes were then deleted in the strains AKD228 and *TPK2*-GFP by PCR-mediated gene deletion using the oligonucleotide pairs ccz1Δ_F/ccz1Δ_R and sap30Δ_F/sap30Δ_R and pUG72 as template (7). The deletion of the same genes was performed in the BY4742 strain, and the strains were then crossed with AKD228 and the *TPK2*-GFP strain harboring the same deletion and were selected on SC-Met/Lys, leading to the strains AKD231, AKD232, AKD237, and AKD238. Cells in stationary phase (24 h of preculture) were diluted to an OD_{600}/mL of 0.1 in SC/PCA-Ade/Met/Lys and were grown until they reached an OD_{600} of 0.5–0.6. The equivalent of 25 OD_{600} of cells was collected and processed to perform the coimmunoprecipitation of the *BCY1*-GFP/*TPK2*-6HA strains with GFP-Trap_M (Chromotek) as described by the distributor. For the *TPK2*-GFP strains, the equivalent of 75 OD_{600} of cells was collected and processed to perform the coimmunoprecipitation with the same system. At least three independent cultures and coimmunoprecipitations were performed for each deletion strain. Pixel quantification of lysate and eluate was performed using ImageStudio lite (Odyssey FC; LI-COR). A technical replicate of the wild type was used to normalize between gels.

Genetic Interactions Between the Ras/cAMP/PKA Pathway and PKA Regulator Candidates. Plasmid pPHY921 (kindly provided by Paul Herman) carrying a hyperactive allele of *RAS2* (*RAS2*^{Val19}) (8) or the control plasmid pRS316 was transformed in strains from the Yeast Knock-Out collection (4), including *ho*Δ as a control. Five colonies of each transformation were grown in 400 μL of SC-Ura for 2 d at 30 °C. Ten microliters of the saturated preculture were placed randomly in a 96-position array on four identical SC-Ura OmniTrays (Thermo Scientific) and were incubated for 2 d at 30 °C. The four arrays were then condensed to form 384 arrays on the scoring medium using a BM3-BC

robot with a 96-pin tool (S&P Robotics Inc.) and were incubated for 4 d at 30 or 37 °C. A standard least-square model testing the interaction between Ras hyperactivation and the deletion was performed independently for each condition. Scores at an FDR threshold <0.05 were reported as significant.

Analysis of Known Regulators and Substrates. The set of kinases that putatively phosphorylate Bcy1, Tpk1, Tpk2, or Tpk3 and the substrates that PKA catalytic subunits may phosphorylate were retrieved from the Kinase Interaction Database (KID) (9). The quantitative KID score reported in the database reflects the level of confidence for each pair. We intersected the list of putative kinases and substrates with our candidates. In addition, PKA transcriptional regulators were retrieved from ref. 10 and intersected with our regulators.

Phenotypic Enrichments. Phenotypic data for response to drugs [retrieved from the Saccharomyces Genome Database (SGD), www.yeastgenome.org, October 2, 2013] and filamentous growth (11), glycogen accumulation (12), and protein acetylation (13) phenotypes were used to compare differences in absolute PKA score among these categories using Wilcoxon's test.

Network Proximity Analysis. Physical (reported by at least two different experimental systems) and genetic interaction data were retrieved from BioGRID 3.2.99 (14) and split into negative genetic, positive genetic, and physical interactions according to BioGRID annotation. The shortest path and the congruency between network member pairs were computed using custom Perl scripts. The shortest path was measured as the smallest number of interactions separating two members, plus one (e.g., a direct interaction has a shortest path of 1, two proteins that do not interact directly but have a common interaction partner have a shortest path of 2, and so forth). The congruency was measured as the proportion of common partners between two members' intersection (i.e., intersection divided by union). Values for each pair of candidate regulators were averaged and compared with a distribution of 100,000 permutations performed by sampling a random set of the same size among all of the 3,726 tested genes, and a Z-score was computed.

Physical and Genetic Interaction Enrichments. Interactions with yeast PKA subunits were retrieved from BioGRID 3.2.99 (14). Enrichment among our candidates was tested with Fisher's exact test.

Physical Interaction with PKA Subunits. A DHFR-PCA screen between Tpk1, Tpk2, and Bcy1 against the DHFR collections was performed (15). The six bait strains (*BCY1*, *TPK1*, and *TPK2* fused to either the DHFR F[1,2] or DHFR F[3] fragments) were retrieved from the two PCA collections. The two yeast DHFR collections (DHFR F[1,2] and DHFR F[3], 4,326 and 4,804 strains, respectively) were grown on four plates in arrays of 1,536 strains, and screens were performed as described in ref. 16 but at this density. These steps were performed in duplicate. Colony sizes were $\log_2$ transformed and adjusted for plate bias by subtracting the plate median and adding the overall assay mean to obtain PCA scores. Growth values were averaged for the two replicates, and, because reciprocal interactions (for instance Bcy1-DHFR F[1,2] × DHFR F[3] and Bcy1-DHFR F[3] × DHFR F[1,2] collection) are not directly comparable (1, 15), only the maximum value between the two reciprocal orientations was reported for each interaction. Interactions were filtered using a list of proteins previously reported to interact with the DHFR fragments (15). Because the strains with the 1% highest interaction scores in each experiment in glucose were enriched in interactors previously reported in BioGRID 3.2.99 (14) (P value <0.05, Fisher's exact test), this threshold was considered to define putative interaction partners to be intersected with the PKA regulators (Dataset S1).

Bcy1 Interactome Mapping by AP Followed by MS. For the TAP experiment, the Bcy1-fusion strain and BY4741 (used as a negative control) were grown overnight in SC-Ade and were diluted to an OD_{600}/mL of 0.1 in fresh medium. When the cultures reached an OD_{600}/mL between 0.5 and 0.7, 500 OD equivalents of cells were harvested, washed in extraction buffer [20 mM Hepes-NaOH (pH 7.4), 300 mM NaCl, 0.1% Nonidet P-40, 2 mM $MgCl_2$, 5% glycerol, 1 mM DTT, 1 mM PMSF, 2 μg/mL leupeptin, 2 μg/mL pepstatin, 5 μg/mL aprotinin, 10 mM sodium butyrate, 10 mM β-glycerophosphate], resuspended in 1 mL of extraction buffer, and frozen in liquid nitrogen and stored at −80 °C. Thawed cells were lysed with glass beads at 4 °C by vortexing five times for 1 min interspersed by 1 min cooling. Lysates were centrifuged for 20 min at 16,100 × g at 4 °C. The supernatant was precleared with 50 μL of CL-6B Sepharose beads (Sigma-Aldrich) equilibrated with extraction buffer and incubated for 45 min at 4 °C on a rotating wheel. Supernatant was incubated with Dynabeads (Life Technology) coupled to rabbit total IgG as described previously (17). Beads were recovered and washed three times. Bcy1-TAP complexes were eluted by 2 h incubation at 4 °C with 13 U of tobacco etch virus (TEV) protease (Invitrogen) in 100 μL of TEV buffer [10 mM Tris·HCl (pH 8.0), 150 mM NaCl, 0.1% Nonidet P-40, 0.5 mM EDTA, 1 mM DTT]. The supernatant was recovered, frozen in liquid nitrogen, and stored at −80 °C. Half of each sample was thawed and incubated overnight at 4 °C with 50 μL of calmodulin affinity resin (Stratagene) in 5 mM of $CaCl_2$. Beads were recovered and washed three times in calmodulin buffer (18) and twice in 10 mM Tris·HCl (pH 8.0). Proteins were eluted with 100 μL of 50 mM H_3PO_4 (pH 1.8) on ice for 10 min. The elution was repeated twice, and the eluates were pooled and stored at −80 °C until tryptic digestion. Samples were processed as previously described (19). One-quarter of each sample was analyzed by MS.

For the GFP AP, the GFP-Bcy1 strain (in duplicate) and BY4741 (used as a negative control) were grown overnight in SC-Ade and diluted to an OD_{600}/mL of 0.1 in fresh medium. When the cultures reached an OD_{600} of 0.5, 50 OD equivalents of cells were harvested in two aliquots for each culture, washed in cold water, flash-frozen in liquid nitrogen, and stored at −80 °C. In the meantime, the cultures were treated with 200 ng/mL of rapamycin (Bioshop), and incubation was prolonged for 3 h. Fifty OD equivalents of cells were harvested in two aliquots for each culture as described above. Each aliquot was then thawed and resuspended in 200 μL extraction buffer [10 mM Tris·HCl (pH 7.5), 150 mM NaCl, 0.5 mM EDTA, 0.1% Tween-20, protease inhibitor (Complete Mini Roche), and phosphatase inhibitor (PhosSTOP)]. Cells were lysed at 4 °C with glass beads by vortexing 10 times for 30 s interspersed by 1 min cooling. Cell lysates were recovered by centrifugation at 16,100 × g at 4 °C in a 5415R Centrifuge (Eppendorf) for 5 min. The two aliquots were combined, and 100 μL of dilution buffer [10 mM Tris·HCl (pH 7.5), 150 mM NaCl, 0.5 mM EDTA] was added. Thirty microliters of magnetic beads (GFP-Trap_M; Chromotek) pretreated according to the manufacturer's protocol were added and incubated for 2 h at 4 °C on a wheel. Beads were washed three times with ice-cold dilution buffer and twice with ice-cold buffer [10 mM Tris·HCl (pH 7.5)]. Protein complexes were eluted three times by incubation at 4 °C with 100 μL of 50 mM H_3PO_4, and the three elutions were pooled. Samples were digested as previously described (19).

MS experiments were performed at the Proteomics platform of the Centre Hospitalier Universitaire de Québec Research Center, Quebec, Canada. A TripleTOF 5600 mass spectrometer equipped with a nanospray III ion source (AB Sciex) and coupled

to a 1200 Nanopump (Agilent) was used for analyses. Mass spectra were acquired using a data-dependent acquisition mode using Analyst software version 1.6 (AB Sciex). Tandem mass spectra were extracted, charge state deconvoluted, and deisotoped in ProteinPilot version 4.5 (AB Sciex). All MS/MS samples were analyzed using Mascot (Matrix Science) and/or X! Tandem (GPM, www.thegpm.org) and were set up to search the UniRef 100 (March 2013) *S. cerevisiae* database (35,320 entries). Peptide mass tolerance was set at 0.1 Da, and fragment mass tolerance was set to 0.1 Da. Scaffold (Proteome Software Inc.) was used to validate MS/MS-based peptide and protein identifications. Peptide identifications generally were accepted if they could be established at greater than 95.0% probability as specified by the Peptide Prophet algorithm (20). Proteins that contained similar peptides but that could not be differentiated based on MS/MS analysis alone were grouped to satisfy the principles of parsimony. Significance analysis of interactome (SAINT) was performed via the CRAPome website (www.crapome.org) (21–23) using the *S. cerevisiae* database via workflow 3 (CRAPome v1.1). AP-MS negative controls (as described above) were combined with CRAPome controls (CC519-531 for GFP AP, CC515-531 for TAP) to create virtual controls for each analysis. Default parameters were used for SAINTexpress. Proteins considered as true interactors and included in the final lists had a SAINT score ≥0.8 (Datasets S1, S3, and S4).

Gene Ontology Enrichment. Gene ontology (GO) enrichments were computed using the Fisher's exact test implemented in Go-elite v. 1.2.5 (24) using default settings and a minimum of two genes per ontology category. Enrichments were calculated for each list of candidates determined in each screen (positive or negative, PKA1- or PKA2-specific, direct candidates, and so forth). GO Slim cellular components were obtained from SGD, and a custom cellular map was created using JMP10 (SAS Institute) onto which average PKA scores were mapped. Enrichment *P* values were calculated based on the distribution of 10,000 randomizations.

Protein Complex Analysis. The Protein Complex-Based Analysis Framework for High-Throughput Data Sets (COMPLEAT) online application (25) was used to compute enrichment *P* value and interquartile mean score for our dataset. *P* values were estimated using 1,000 permutations of the complex composition.

Comparison of Autophagy Induction in Different Media. Plasmid pRS316 [GFP-ATG8] (kindly provided by Daniel Klionsky, Life Sciences Institute, University of Michigan, Ann Arbor, MI) (26) was transformed in BY4741 and selected on SC-Ura plates for 2 d at 30 °C. Two transformants were grown overnight at 30 °C in 10 mL of SC-Ura. The next day, 50 mL of SC-Ura were inoculated at an OD_{600} of 0.003 and incubated at 30 °C overnight. The next morning, when the cultures had reached an OD_{600} of ∼1, 55 mL of SC-Ura were inoculated to an OD_{600} of 0.25 and were incubated for 4 h at 30 °C. Cells were then washed with sterile water and resuspended in 5.5 mL of sterile water. One hundred microliters of cells were used to measure OD; 400 μL of cells were harvested by centrifugation for 1 min at 16,100 × *g* in a Centrifuge 5415R (Eppendorf) and stored at −80 °C (t_0); and 500 μL of cells were used to inoculate three 13-mL tubes of each of three different autophagy induction media: the autophagy-induction medium (1.7% yeast nitrogen base without ammonium sulfate and without amino acids, 2% glucose), the SC/PCA medium, and the SC/PCA medium supplemented with 0.1 g/L methionine. Cellular extracts were prepared and adjusted according to the OD of the culture and were analyzed by Western blot as described previously (5) with a mouse anti-GFP primary antibody (11 814 460 001; Roche) and a goat anti-mouse IgG secondary antibody (IRDye 800, LIC-926-32210; Mandel Scientific). Image pixel quantification was performed using ImageStudio lite (LICOR Odyssey), and autophagic flux was calculated as the cleaved GFP proportion of the total GFP signal (GFP + GFP-Atg8).

PKA Assays and DHFR-PCA with Methionine and Rapamycin. A small-scale PKA assay for selected manually reconstructed strains (described above) was performed in MTX/Glu and DMSO/Glu supplemented with methionine (0.1 g/L), rapamycin (2.5 ng/mL), or both. Reported protein interactions involving Bcy1 and other interactions relevant to autophagy and methionine signaling were also tested by DHFR-PCA, as described above, on the same media (Dataset S7). All strains were printed in eight replicates, excluding those on border positions on agar plates, at a density of 1,536 colonies per plate using a BM3-BC robot (S&P Robotics, Inc.). The difference in ranked colony size on MTX/Glu and DMSO/Glu media was computed, and the median of 10 time points (20–140 h) was then used as the ranked difference for each biological replicate. For PKA assays, rank differences of deletion strains were also centered by the medians of their respective ZL–ZL controls. For DHFR-PCA, a normal two-mixture fit was used to report positive protein interactions (score >0.5) (Dataset S7). Each condition pair was tested with a *t* test, and multiple testing was accounted for by an FDR *P* value adjustment. Known interactions that were weakly detected by DHFR-PCA (score <0.5) but were significantly modulated between conditions (FDR <0.05) were also reported (Dataset S7).

Rluc PCA in Mammalian Cells. A stable HEK293 cell line coexpressing the PCA hybrid proteins RIIβ-Rluc-F[1] and PKAc-RlucF[2] (PCA-based PKA reporter) was used as previously described (27, 28). Further, the PKA homodimer hybrid proteins RIIβ-*R*lucF[1] and RIIβ-*R*lucF[2] were transiently overexpressed in HEK293 cells using the general cell transfection reagent Transfectin (Bio-Rad). Using a site-directed mutagenesis protocol, we exchanged K285 and K293 with R or Q to generate RII (K285/293R)-RlucF[1] and RII(K285/293Q)-RlucF[1]. Combinations of PKA hybrid proteins RIIβ-RlucF[1], RIIβ-RlucF[2], RII(K285/293R)-RlucF[1], RII(K285/293Q)-RlucF[1], and PKAc-RlucF2 were transiently overexpressed in HEK293 cells using Transfectin. In indicated experiments, specific acetyltransferases [PCAF and TIP60 (29, 30)] were transiently overexpressed in the PCA-PKA reporter cell line. All cells were grown in DMEM (Invitrogen) supplemented with 10% FBS in 24-well plates. At 24 h or 48 h after transfection or seeding, confluent cells were treated with 20 μM Forskolin and equal volumes of the solvent (ethanol) or with 1 μM TSA for 3 h at 37 °C. After treatments, the growth medium was exchanged, and cells were resuspended in PBS. Cell suspensions were transferred to 96-well plates and were subjected to bioluminescence analysis using the LMaxII^{384} luminometer (Molecular Devices). Rluc bioluminescence signals were integrated for 10 s following the addition of the Rluc substrate benzyl-coelenterazine (5 μM; Nanolight). Bioluminescences measured for the RC and RR complex upon TSA treatment were normalized by the ethanol control and compared using Welch's test. Signals obtained for RC complex when PCAF and TIP60 were overexpressed were normalized by the expression of either the R or C subunit (Fig. S7) and were compared with the mock control using log-transformed data with a blocked Dunnett's test. Signals obtained for RII(K285/293R)-RlucF[1] and RII(K285/293Q)-RlucF[1] were compared uisng a blocked Welch's test.

cAMP Agarose Protein Precipitation Assay. HEK293 cells transiently expressing either TIP60-HA or PCAF-Flag were homogenized using a Potter S laboratory mixer (B. Braun Biotech International) with 15 strokes [lysis buffer: 10 mM sodium phosphate (pH 7.2), 150 mM NaCl, 0.05% Triton X-100 supplemented with standard protease inhibitors]. The lysate was clarified (15,700 × *g* for 15 min), and protein complexes associated with the PKA

regulatory subunit were precipitated with PKA-selective Rp-8-AHA-cAMP agarose resin (D014 and M012; Biolog) for 2 h at 4 °C to isolate endogenous PKA holoenzymes. As a negative control experiment, excess cAMP (5 mM) was added to the lysate to mask the cAMP-binding sites in the R subunits for precipitation. Resin-associated proteins were washed four times with lysis buffer and eluted with Laemmli sample buffer. Proteins were subjected to PAGE followed by immunoblotting with commercially available antibodies versus PKA subunits RIIb and PKAc (28), α-tubulin, and the HA and FLAG tags. As a negative control, immunoblots from all experiments were stripped and reprobed with α-tubulin antibody (T5168; Sigma-Aldrich).

Construction of Bcy1 Acetylation Mutants. To mutate Bcy1 lysines of interest to arginine or glutamine, in vitro mutagenesis of the wild-type allele of *BCY1* carried by plasmid pJS11 (kindly provided by Yolanda Sanchez, Dartmouth Medical School, Hanover, NH) (31) was performed according to the procedure indicated in the QuikChange site-directed mutagenesis kit (Stratagene). Oligonucleotides (Dataset S9) containing the appropriate mutation were used to amplify the plasmid by PCR. The PCR product was then digested with Dpn I and transformed in bacteria. Plasmids were Sanger-sequenced to confirm the mutations. Plasmids carrying the mutated alleles of *BCY1* were transformed into a *bcy1*Δ strain following a five-step procedure because of inefficient transformation in a standard *bcy1*Δ strain. A *bcy1*Δ strain (FTQ036), constructed by PCR-mediated deletion of *BCY1* (oligonucleotides bcy1Δ_F and bcy1Δ_R on plasmid pUG6) (7) and confirmed by colony PCR (oligonucleotides KanB_R and bcy1_A), was mated with BY4742 transformed with pMoBY-*BCY1* from the MoBY collection (32), and the diploid was selected on SC-Met/Lys/Ura. After sporulation and tetrad dissection, an MATa haploid strain carrying both the *bcy1*Δ genomic allele and the pMoBY-*BCY1* plasmid was selected and confirmed by colony PCR, leading to strain IGA43. This strain was then transformed with the different plasmids carrying the mutated alleles of *BCY1*, with the original plasmid, pJS11, carrying the wild-type allele, and with pYCJ1 and pYCJ2 carrying an allele of *BCY1* mutated at its cluster of phosphorylation sites (31). All the resulting strains were then streaked on 5-fluoroorotic acid (5-FOA) to select for cells that had lost the pMoBY-*BCY1* plasmid. The resulting strains hence expressed only a mutated allele of *BCY1*.

Glycogen Staining of Bcy1 Mutants. Strains carrying *BCY1* mutant alleles were grown in SC-Leu. The OD_{600}/mL was adjusted to 1, and 5 μL were spotted on SC-Leu and YPD + G418 and were incubated for 48 h at 30 °C. Strains were stained with iodine vapors by filling a Petri lid with crystalline iodine and placing the Petri dish upside-down on top of the lid. After 10 min of coloration, the Petri dishes were allowed to fade, and pictures were taken after 2.5, 5, and 10 min of discoloration.

Chronological Lifespan of Bcy1 Mutants. The chronological lifespan of *BCY1* Q and R mutants of K313 and K313,321 and of a wild-type control (pJS11) was measured as described in ref. 33 for six biological replicates. Survival percentage and the area under the survival curve were also calculated as described. The Tukey–Kramer HSD method was used to test for significant differences between strains.

1. Diss G, Dubé AK, Boutin J, Gagnon-Arsenault I, Landry CR (2013) A systematic approach for the genetic dissection of protein complexes in living cells. *Cell Reports* 3(6):2155–2167.
2. Costanzo M, et al. (2010) The genetic landscape of a cell. *Science* 327(5964):425–431.
3. Leducq JB, et al. (2012) Evidence for the robustness of protein complexes to interspecies hybridization. *PLoS Genet* 8(12):e1003161.
4. Giaever G, et al. (2002) Functional profiling of the *Saccharomyces cerevisiae* genome. *Nature* 418(6896):387–391.
5. Freschi L, Torres-Quiroz F, Dubé AK, Landry CR (2013) qPCA: A scalable assay to measure the perturbation of protein-protein interactions in living cells. *Mol Biosyst* 9(1):36–43.
6. Janke C, et al. (2004) A versatile toolbox for PCR-based tagging of yeast genes: New fluorescent proteins, more markers and promoter substitution cassettes. *Yeast* 21(11): 947–962.
7. Güldener U, Heck S, Fielder T, Beinhauer J, Hegemann JH (1996) A new efficient gene disruption cassette for repeated use in budding yeast. *Nucleic Acids Res* 24(13):2519–2524.
8. Ramachandran V, Herman PK (2011) Antagonistic interactions between the cAMP-dependent protein kinase and Tor signaling pathways modulate cell growth in *Saccharomyces cerevisiae*. *Genetics* 187(2):441–454.
9. Sharifpoor S, et al. (2011) A quantitative literature-curated gold standard for kinase-substrate pairs. *Genome Biol* 12(4):R39.
10. Venters BJ, et al. (2011) A comprehensive genomic binding map of gene and chromatin regulatory proteins in Saccharomyces. *Mol Cell* 41(4):480–492.
11. Ryan O, et al. (2012) Global gene deletion analysis exploring yeast filamentous growth. *Science* 337(6100):1353–1356.
12. Wilson WA, Wang Z, Roach PJ (2002) Systematic identification of the genes affecting glycogen storage in the yeast *Saccharomyces cerevisiae*: Implication of the vacuole as a determinant of glycogen level. *Mol Cell Proteomics* 1(3):232–242.
13. Henriksen P, et al. (2012) Proteome-wide analysis of lysine acetylation suggests its broad regulatory scope in *Saccharomyces cerevisiae*. *Mol Cell Proteomics* 11(11):1510–1522.
14. Chatr-Aryamontri A, et al. (2013) The BioGRID interaction database: 2013 update. *Nucleic Acids Res* 41(Database issue):D816–D823.
15. Tarassov K, et al. (2008) An in vivo map of the yeast protein interactome. *Science* 320(5882):1465–1470.
16. Gagnon-Arsenault I, et al. (2013) Transcriptional divergence plays a role in the re-wiring of protein interaction networks after gene duplication. *J Proteomics* 81:112–125.
17. Mitchell L, et al. (2008) Functional dissection of the NuA4 histone acetyltransferase reveals its role as a genetic hub and that Eaf1 is essential for complex integrity. *Mol Cell Biol* 28(7):2244–2256.
18. Puig O, et al. (2001) The tandem affinity purification (TAP) method: A general procedure of protein complex purification. *Methods* 24(3):218–229.
19. Bisson N, et al. (2011) Selected reaction monitoring mass spectrometry reveals the dynamics of signaling through the GRB2 adaptor. *Nat Biotechnol* 29(7):653–658.
20. Keller A, Nesvizhskii AI, Kolker E, Aebersold R (2002) Empirical statistical model to estimate the accuracy of peptide identifications made by MS/MS and database search. *Anal Chem* 74(20):5383–5392.
21. Teo G, et al. (2014) SAINTexpress: Improvements and additional features in Significance Analysis of INTeractome software. *J Proteomics* 100:37–43.
22. Mellacheruvu D, et al. (2013) The CRAPome: A contaminant repository for affinity purification-mass spectrometry data. *Nat Methods* 10(8):730–736.
23. Choi H, et al. (2011) SAINT: Probabilistic scoring of affinity purification-mass spectrometry data. *Nat Methods* 8(1):70–73.
24. Zambon AC, et al. (2012) GO-Elite: A flexible solution for pathway and ontology over-representation. *Bioinformatics* 28(16):2209–2210.
25. Vinayagam A, et al. (2013) Protein complex-based analysis framework for high-throughput data sets. *Sci Signal* 6(264):rs5.
26. Yi C, et al. (2012) Function and molecular mechanism of acetylation in autophagy regulation. *Science* 336(6080):474–477.
27. Stefan E, et al. (2007) Quantification of dynamic protein complexes using Renilla luciferase fragment complementation applied to protein kinase A activities in vivo. *Proc Natl Acad Sci USA* 104(43):16916–16921.
28. Bachmann VA, et al. (2013) Reciprocal regulation of PKA and Rac signaling. *Proc Natl Acad Sci USA* 110(21):8531–8536.
29. Legube G, et al. (2002) Tip60 is targeted to proteasome-mediated degradation by Mdm2 and accumulates after UV irradiation. *EMBO J* 21(7):1704–1712.
30. Yang XJ, Ogryzko VV, Nishikawa J, Howard BH, Nakatani Y (1996) A p300/CBP-associated factor that competes with the adenoviral oncoprotein E1A. *Nature* 382(6589):319–324.
31. Searle JS, Wood MD, Kaur M, Tobin DV, Sanchez Y (2011) Proteins in the nutrient-sensing and DNA damage checkpoint pathways cooperate to restrain mitotic progression following DNA damage. *PLoS Genet* 7(7):e1002176.
32. Ho CH, et al. (2009) A molecular barcoded yeast ORF library enables mode-of-action analysis of bioactive compounds. *Nat Biotechnol* 27(4):369–377.
33. Murakami C, Kaeberlein M (2009) Quantifying yeast chronological life span by outgrowth of aged cells. *JoVE* (27):e1156.

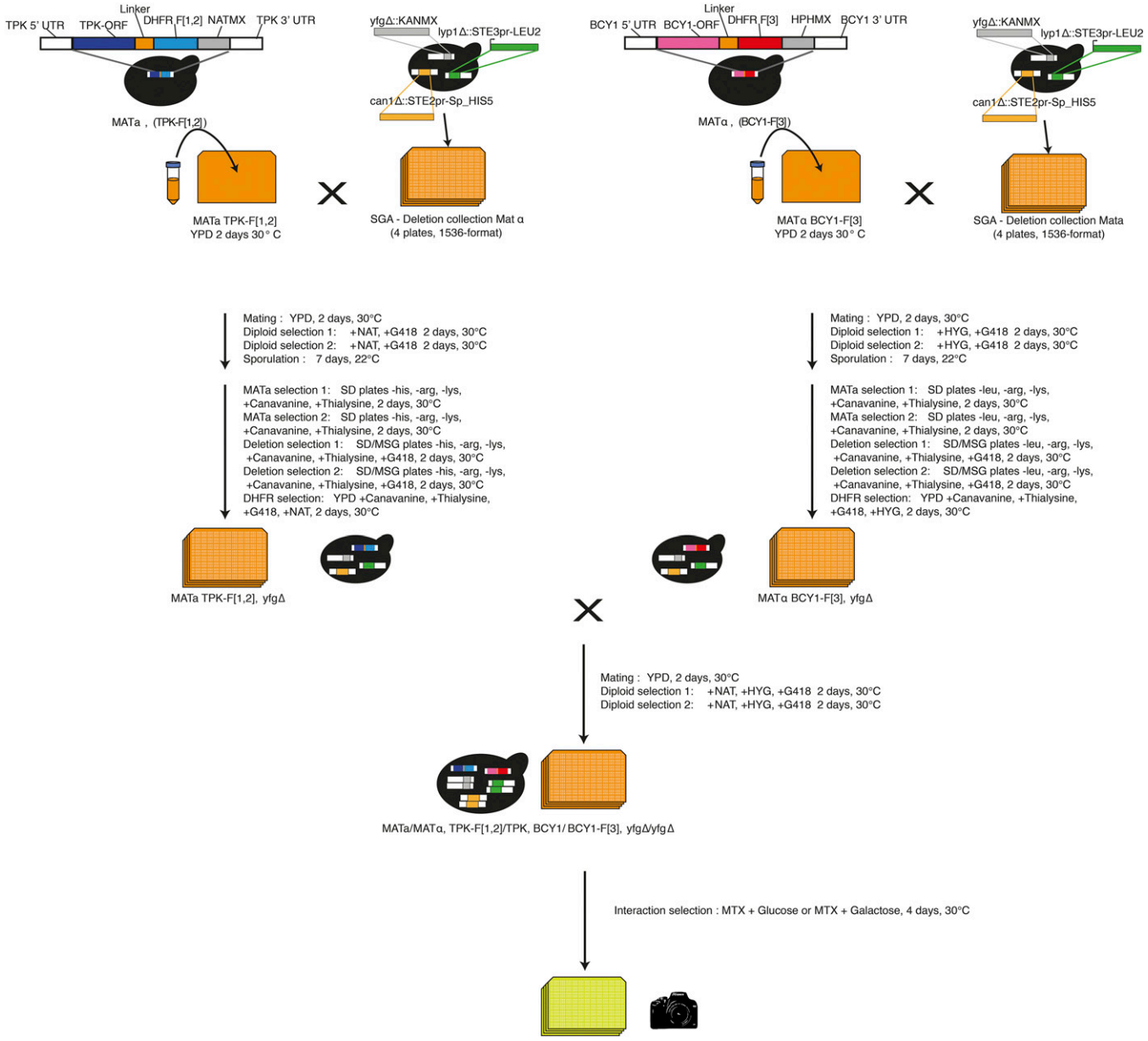

Fig. S1. PKA assay screening method. Yeast collections were assembled on four solid YPD + G418 plates in arrays of 1,536 colonies and were grown on 5-FOA plates to select for cells that had lost the pRS316 plasmid. The collections were printed on YPD plates, and saturated cultures of the PCA strains were printed on top and incubated for 48 h at 30 °C. Strain *BCY1*-DHFR F[3] was mated with the *MAT**a*** SGA-ready deletion collections (4), and strains *TPK1*-DHFR F[1,2] and *TPK2*-DHFR F[1,2] were each mated with the *MAT**α*** collection. Each mating was performed in four replicates. Several strains containing the *BCY1*-DHFR F[3] fusion did not produce recombinant genotypes at this stage (70 ± 2.2% successful on average). Therefore, we combined the four replicates of *BCY1*-DHFR F[3] to get a more complete coverage. We obtained one collection with 87.98% of the strains. Haploid yeast deletion collections expressing the complementary DHFR fragments (each with the same deletion at the same position on 1,536 arrays) were crossed to perform the PKA assays. The *MAT**a*** collections (*TPK1*-DHFR F[1,2] *yfg*Δ or *TPK2*-DHFR F[1,2] *yfg*Δ) and the *MAT**α*** collection (*BCY1*-DHFR F[3] *yfg*Δ) were replicated on the same YPD plate and incubated for 48 h at 30 °C. Diploid cells were selected twice on sel2n2 medium for 48 h at 30 °C. This selection allowed us to obtain diploid cells heterozygous for each DHFR fragment (*TPK1*-DHFR F[1,2]/*TPK1 BCY1*/*BCY1*-DHFR F[3] or *TPK2*-DHFR F[1,2]/*TPK2 BCY1*/*BCY1*-DHFR F[3]) and homozygous for the deletion of one gene (*yfg*Δ/*yfg*Δ). As a result of the strain-construction process, 16 plates of homozygous deletion strains in four replicates were obtained for each interaction measured. To measure the interactions on different carbon sources, each of these plates was replicated on MTX/Glu and MTX/Gal media and incubated at 30 °C. Pictures of plates were taken after 48 and 96 h of growth using a 10.1-megapixel camera (EOS Rebel XS; Canon) equipped with a polarizing filter. *yfg*, your favorite gene.

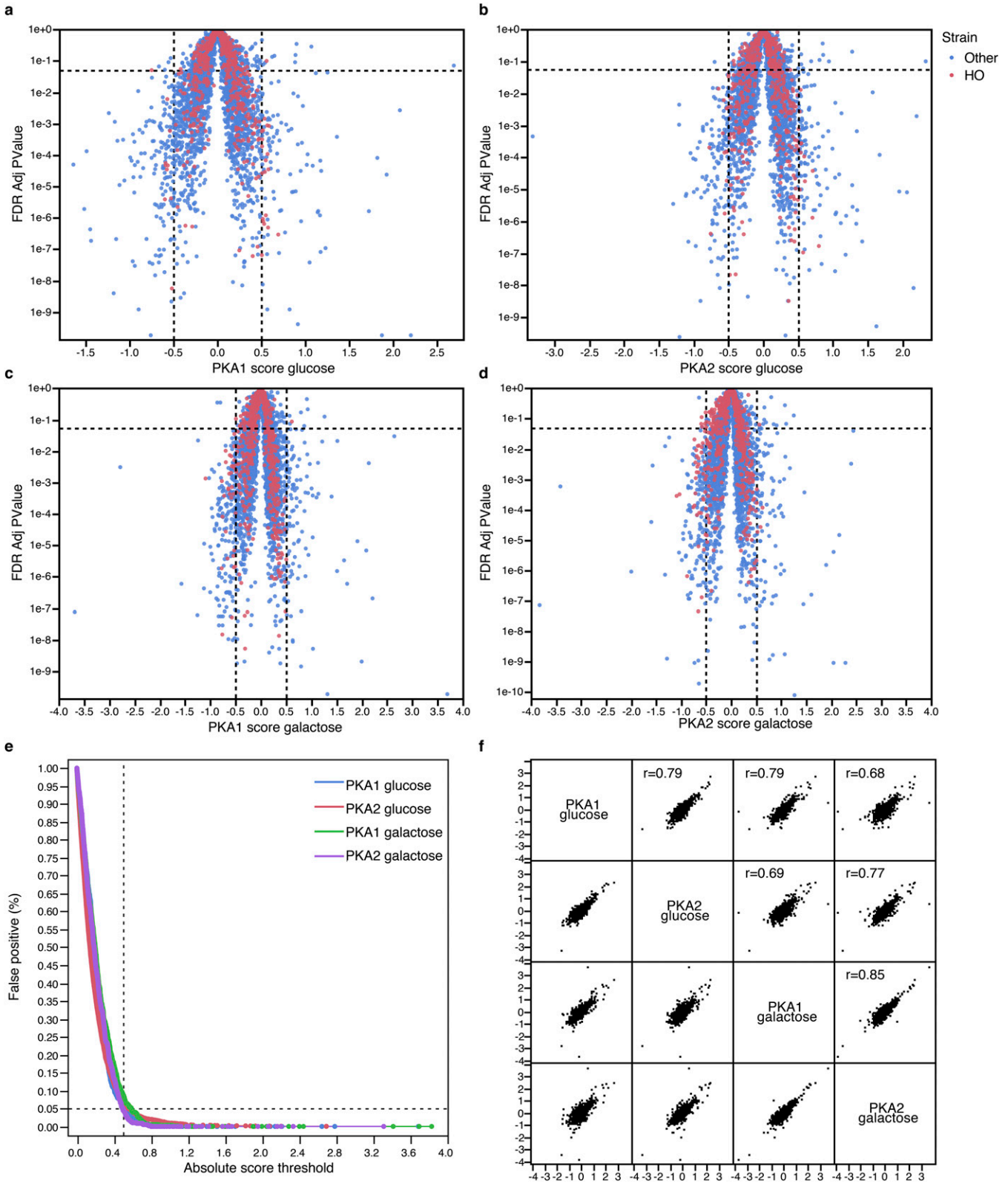

Fig. S2. Results of the four PKA assays (related to Fig. 1*C* and Dataset S1). (*A*–*D*) The *x* axis shows the score for strain on the plate, and the *y* axis shows the FDR-adjusted *P* value of Welch's test which corresponds to the confidence that the score is different from that of the ZL–ZL control. Red dots represent the *ho*Δ strains, and the blue dots represent the other deletion strains. Dotted lines indicate the selected thresholds. (*E*) The proportion of false-positive results (*ho*Δ positions) is similar among assays with respect to the absolute threshold setting. Overall, 28, 26, 23, and 44 *ho*Δ control positions out of 602, 611, 614, and 611, respectively, were false positives for PKA1 in glucose and PKA2 in galactose, corresponding to an empirical false-positive rate between 3.7 and 7.2%. (*F*) Correlation between PKA scores; *r* = Pearson correlation.

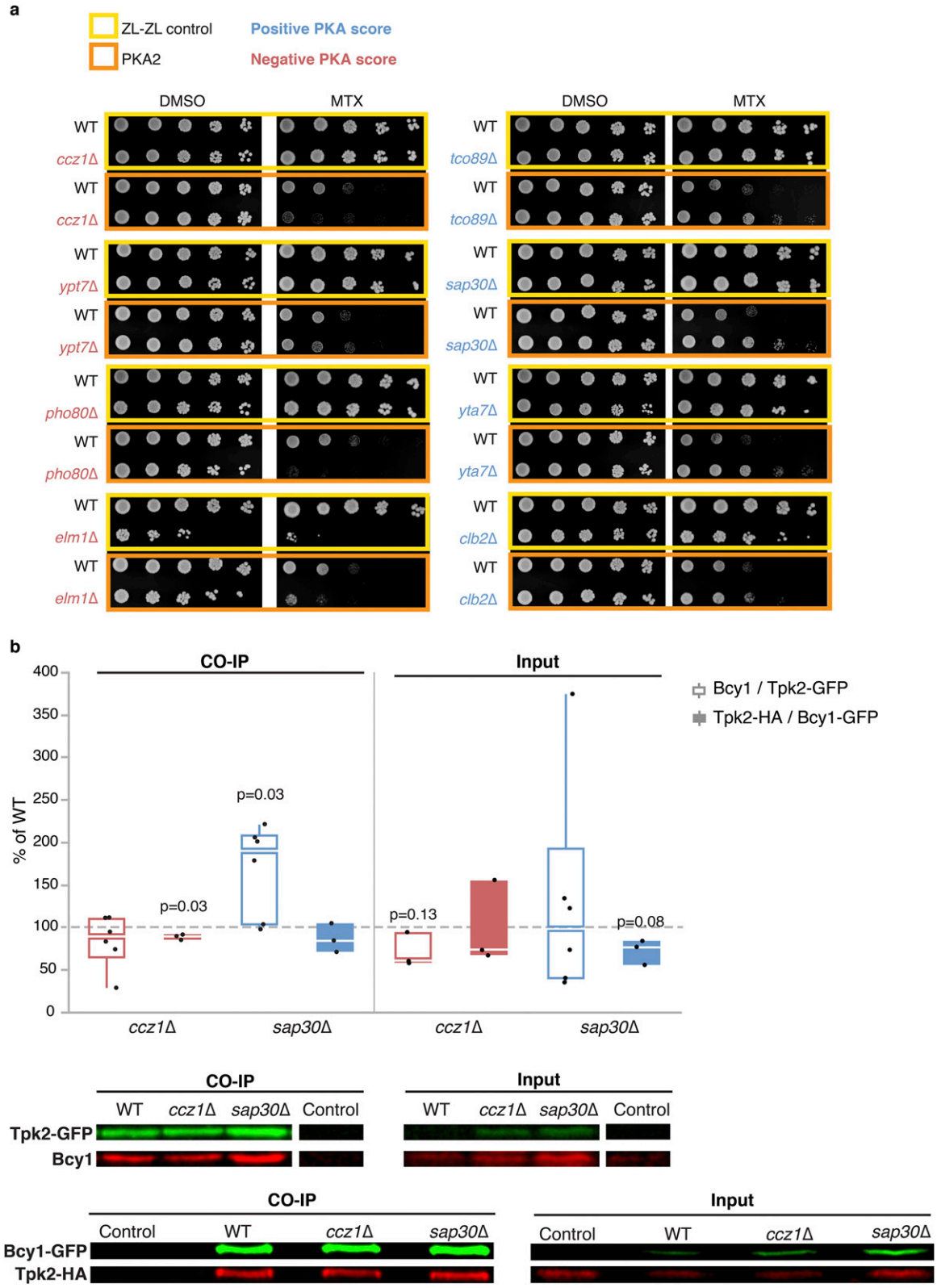

Fig. S3. Confirmation experiments. (*A*) Examples of spot dilution assay of PKA2 assay in glucose (MTX) for eight PKA regulators are displayed along with their ZL–ZL control. Also shown is the growth of strains in a control condition (DMSO). The wild-type strain is *ho*Δ. (*B*) Interaction between Tpk2-HA and Bcy1-GFP and Tpk2-GFP and Bcy1 in *ccz1*Δ and *sap30*Δ relative to wild type by coimmunoprecipitation (GFP-trap beads). The coimmunoprecipitation results confirm the results of the PKA2 assay in each deletion mutant, but in one direction only (two-tailed *P* value; *t* test that mean is different from 100%). When the expected change is not significant, a marginal difference in subunit ratios is observed in the input protein extract, suggesting that the fusion proteins may affect the abundance of the proteins.

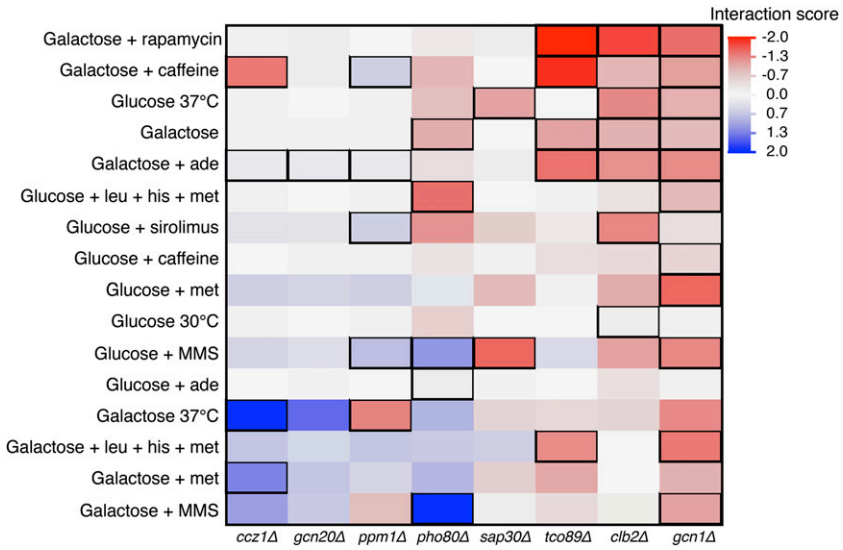

Fig. S4. Deletion of candidate regulator genes can aggravate or compensate for the effect of PKA hyperactivation (*RAS2*^{Val19}) on fitness. The color scale reflects the strength and direction of the interaction score (parameter estimate of standard least-squares model). A positive score indicates that the deletion alleviates the phenotypic consequences of PKA hyperactivation, and a negative score indicates an aggravation. Interaction scores at an FDR threshold of <0.05 are boxed. Deletion of candidate regulator genes shows varying profiles of interactions, confirming a functional link with the RAS pathway. For *ccz1*Δ, *ppm1*Δ, and *pho80*Δ, changes in score from positive to negative in various environmental conditions indicate that these genes may play a role in PKA regulation in response to specific environmental cues. This role is in line with the variation seen between glucose and galactose in the PKA assay.

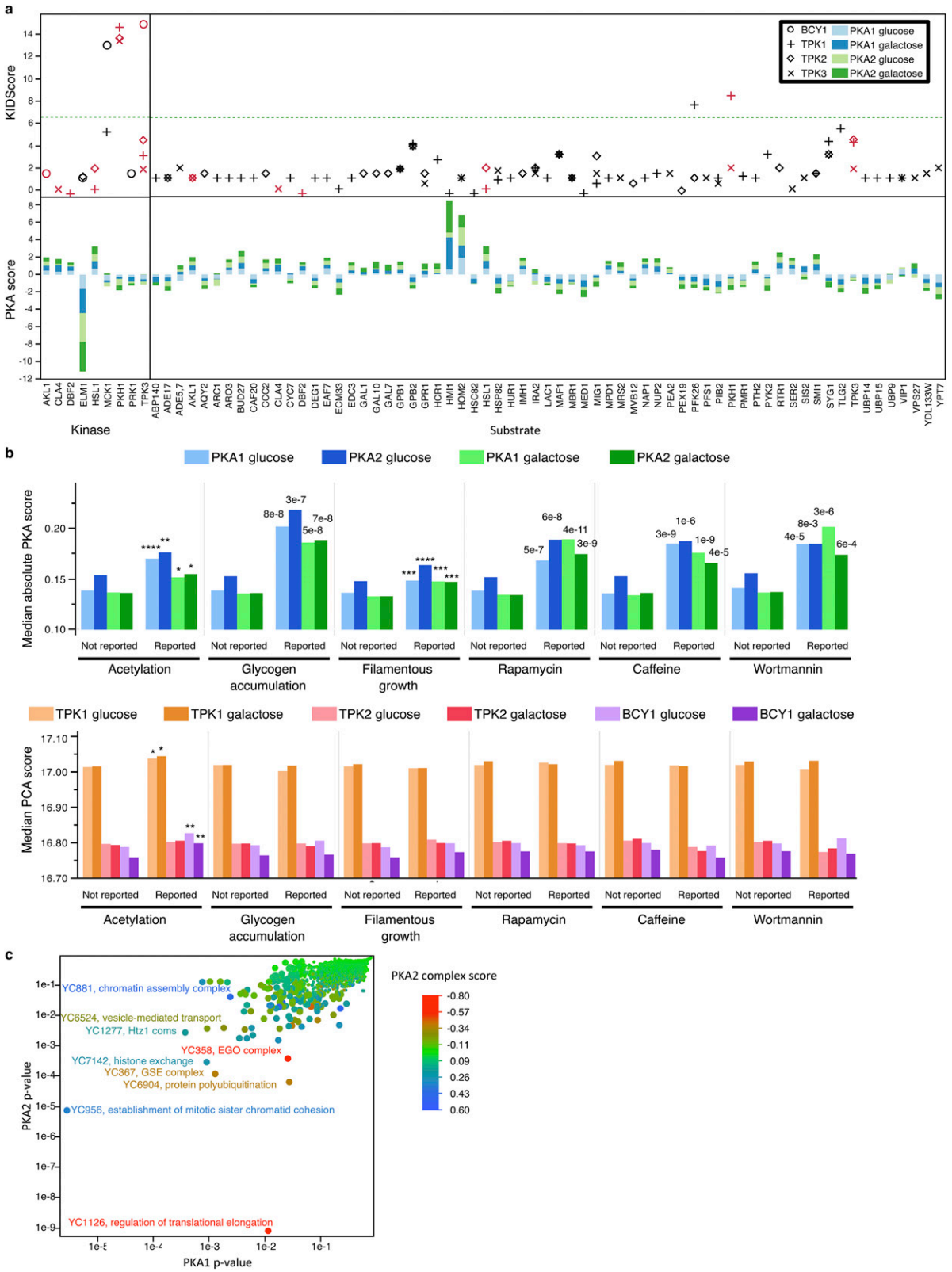

Fig. S5. Intersection of PKA scores with other datasets. (*A*) Kinase–substrate pairs involving any PKA subunit (marked with symbols) and high-confidence candidate regulators (*x* axis). Kinase-phosphorylating PKA subunits are shown on the left, and substrates of PKA are shown on the right. The upper scale shows the KIDScore; the dotted green line represents the gold-standard threshold reported for kinase–substrate pairs (9). Red symbols highlight candidates characterized by bidirectional phosphorylation. The lower scale shows stacked PKA scores (related to Dataset S2). (*B*) Reported *P* values indicate a significant difference in score between reported vs. unreported phenotype. **P* < 0.05, ** *P* < 0.01, **** *P* < 0.0001 (Wilcoxon's test) (related to Fig. 2*C*). (*C*) Results of protein complex enrichment for PKA1 and PKA2 in glucose. Most significant complexes are labeled. The color reflects the interquartile mean of the PKA2 score for the complex. See also Dataset S6.

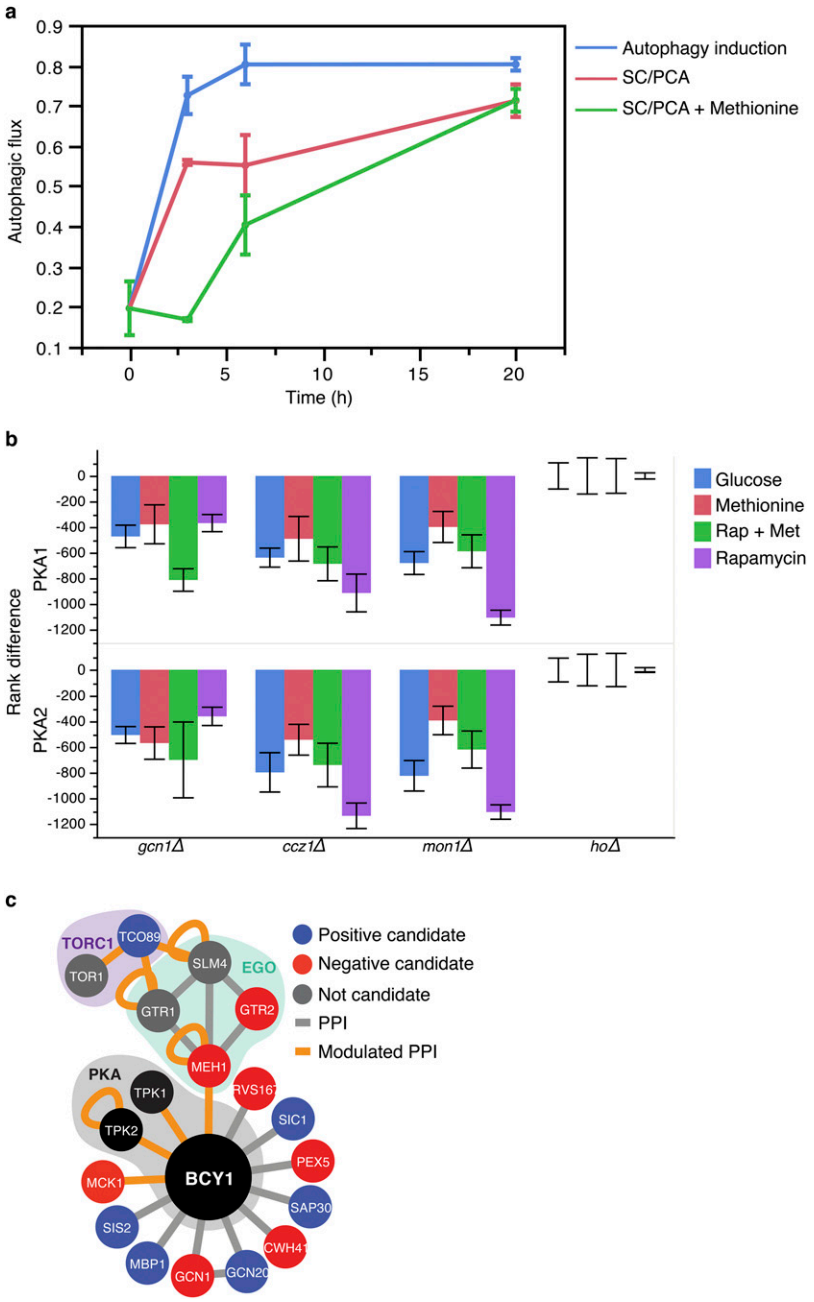

Fig. S6. Interplay between autophagy, methionine, and PKA. (*A*) Induction of autophagy in the PCA medium with and without methionine compared with standard autophagy induction medium. Error bars are 1 SD from the mean of three biological replicates. The results show that in the PKA assay, autophagy is induced in part by the lack of methionine in the medium. (*B*) PKA assay in presence of methionine and/or rapamycin in the deletion strains compared with *ho*Δ strain in the respective condition. The PKA score is measured in a nonparametric fashion with growth rank difference from control to allow comparison among conditions. Negative rank differences indicate less growth than the control in the survival assay, i.e., decreased PKA complex formation. Overall the results support a complex interplay between methionine, TOR, autophagy, and *GCN1* in PKA regulation and suggest that methionine signaling to PKA may occur via multiple paths (related to Fig. 4). (*C*) Bcy1 interactions with candidate regulators as well as interactions within the EGO and TORC1 complex are modulated by methionine and/or rapamycin, as shown by a small-scale DHFR-PCA assay, $n = 8$ (*t* test, FDR <0.05) (related to Dataset S7).

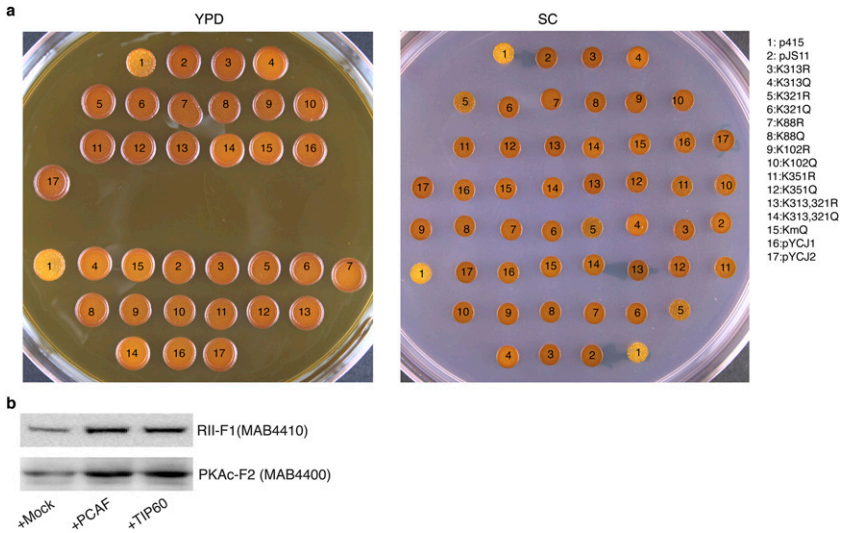

Fig. S7. Follow-up experiments on protein acetylation of the PKA regulatory subunit. (*A*) Glycogen accumulation in yeast Bcy1 mutants compared with wild type (pJS11), *bcy1*Δ (p415), and *bcy1* phosphorylation cluster mutants (pYCJ1 and pYCJ2). Strains that accumulate glycogen appear darker (related to Fig. 6*B*). (*B*) Overexpression of PCAF or TIP60 leads to increased PKA expression in human cells. Both R (MAB4410) and C (MAB4400) subunits show an increase in expression compared with the mock control. $n = 5$ (related to Fig. 5*C*).

Table S1. Candidates with a previously reported relationship to PKA

Relationship to PKA	Candidate genes	Ref.
Ras/cAMP pathway		(1)
Via Ras proteins	*IRA2, TFS1*	
Via Gpa2	*GPR1, RGS2, ASC1*	
Via both	*GPB1, GPB2*	
Transcriptional regulators	*OTU1, IOC4, SKN7, STP1, PHO2, ASF1, RTT103, SWR1, VPS72*	(2)
Genetic interactors (*BCY1, TPK1, TPK2 or TPK3*)	*EDE1, TPS1, ARF1, SWI5, NUM1, SAC3, RVS167, VPS72, SLX8, COG7, SGF73, YGL235W, ICE2, HOM6, YKL069W, SIC1, ATP10, NUP188, BCH1, JNM1, EOS1, HMI1, DIA2, VPS21, GPB1, UBP14, PMR1, HSC82, PHO80, TLG2, GAL7, GAL10, GAL1, GPR1, SWI4, MIG1, YDJ1, IRA2, GPB2, PPM1, SER2, MBR1, HSL1, TPK3, UPS1, VPS71, CTK3, CLA4, HSP82*	(3)
Physical interactors (*Bcy1, Tpk1, Tpk2 or Tpk3*)	*RVS167, ELM1, PTH2, ARO3, EDC3, CYC7, UBP9, DEG1, BUD27, PIB2, ARC1, HUR1, SYG1, LAC1, NAP1, HCR1, UBP15, EAF7, TLG2, ABP140, CAF20, MPD1, PEX19, RTR1, PFK26, PYK2, GPB2, AKL1, HOM2, PKH1, ADE5,7, PFS1, MBR1, HSL1, TPK3, SIS2, VIP1, YPT7, ADE17, VPS27, MRS2, HSP82*	
Kinases	*MCK1, PKH1, TPK3, AKL1, CLA4, DBF2, ELM1, HSL1, PRK1*	(4)
Substrates	*ABP140, ADE17, ADE5,7, AKL1, AQY2, ARC1, ARO3, BUD27, CAF20, CCC2, CLA4, CYC7, DBF2, DEG1, EAF7, ECM33, EDC3, GAL1, GAL10, GAL7, GPB1, GPB2, GPR1, HCR1, HMI1, HOM2, HSC82, HSL1, HSP82, HUR1, IMH1, IRA2, LAC1, MAF1, MBR1, MED1, MIG1, MPD1, MRS2, MVB12, NAP1, NUP2, PEA2, PEX19, PFK26, PFS1, PIB2, PKH1, PMR1, PTH2, PYK2, RTR1, SER2, SIS2, SMI1, SYG1, TLG2, TPK3, UBP14, UBP15, UBP9, VIP1, VPS27, YDL133W, YPT7*	
Downstream transcriptional targets	*HPC2, SPL2, MSL1, YOR338W, TIF4632, MBP1, TAD1, SPS100, PMT2, MAK31, DLD1, AAD4, HXT3, SAP4, SOL3, URA8, MNN4, COX17, PIG1, EXG1, NUP2, ECM30, YNL217W, YNL320W, CAT5, OYE3, YKR047W, APT1, CAC2, MAC1, GIM3, CAR2, MAL32, YHL005C, MSB4, RPS0A, YDR444W, PEX15, MFT1, YGR022C, YPL067C, YCR102C, IDP1, CTH1, YDR266C, RPL34A, MDR1, COS6, YJR054W, YLR040C, YLR253W, PAU4, ZDS2, YMR010W, MCK1, GLO4, STD1, YOR385W, YAR1, YPR114W, GBP2, URA5, YOR292C, KES1, TFS1, SSO2, ALG5, STP1, RAD17, SHM1, CKA2, LEU3, REC102, KAR5, YAL045C, SEC72, RPS10A, QRI7, NPR2, MAD1, SRB8, CCZ1, MET8, MET3, YLR415C, YPL257W, ECM8, VAM7, ECM1, IPT1, ARO1, YDR248C, MET10, MET13, MET14, MET1, MTD1, YLR290C, IMH1, AMD1, MET2, RTS1, MCM16, MET16, LYS12, ROD1, BIK1, PHO2, RPL22A, HOM3, SHM2, VPS4, UBC12, MAF1, MET28, YLR280C, MCM21, PTK1, PDA1, ADH1, RPS25B, PRK1, DBF2, YHL042W, YBR242W, TOM6, RAD9, GCN1, NUP170, GCN20, TSA1, SUR1, UBA3, VPS8, ASF1, SEC22, CPR8, RVS161, SPT8, CDC73, TPS1, ARF1, NUM1, SAC3, HOM6, YKL069W, SIC1, NUP188, HMI1, VPS21, UBP14, UBP9, PMR1, NAP1, HSC82, UBP15, PHO80, TLG2, CAF20, MPD1, PFK26, YDJ1, IRA2, HOM2, ADE5,7, SER2, HSL1, TPK3, SIS2, YPT7, CTK3, CLA4, VPS27*	(5)
Gene deletion affecting PKA expression levels	*SIS2, SDS3, STP1, RTT109, STB5*	(6)

1. Searle JS, Wood MD, Kaur M, Tobin DV, Sanchez Y (2011) Proteins in the nutrient-sensing and DNA damage checkpoint pathways cooperate to restrain mitotic progression following DNA damage. *PLoS Genet* 7(7):e1002176.
2. Venters BJ, et al. (2011) A comprehensive genomic binding map of gene and chromatin regulatory proteins in Saccharomyces. *Mol Cell* 41(4):480–492.
3. Chatr-Aryamontri A, et al. (2013) The BioGRID interaction database: 2013 update. *Nucleic Acids Res* 41(Database issue):D816–D823.
4. Sharifpoor S, et al. (2011) A quantitative literature-curated gold standard for kinase-substrate pairs. *Genome Biol* 12(4):R39.
5. Robertson LS, Causton HC, Young RA, Fink GR (2000) The yeast A kinases differentially regulate iron uptake and respiratory function. *Proc Natl Acad Sci USA* 97(11):5984–5988.
6. Kemmeren P, et al. (2014) Large-scale genetic perturbations reveal regulatory networks and an abundance of gene-specific repressors. *Cell* 157(3):740–752.

Table S2. Plasmids used in this study

Plasmid name	Construct	Marker	Source
pRS316	39	URA3	(1)
pPHY921	*RAS2*^{Val19}	URA3	(2)
p41-ZL-DHFR[1,2]	Zipper::DHFR F[1,2]	NATMX	(3)
p41-ZL-DHFR[3]	Zipper::DHFR F[3]	HPH	(3)
pAG25-linker-F[1,2]-ADHterm	DHFR F[1,2] PAgTEF1-*natMX*-TAgTEF1	NATMX	(4)
pAG32-linker-F[3]-ADHterm	DHFR F[3] PAgTEF1-*HPH*-TAgTEF1	HPH	(4)
pUG6	loxP-PAgTEF1-*kanMX*-TAgTEF1-loxP	KANMX	(5)
pUG72	loxP-PKlURA3-Kl*URA3*-TKlURA3-loxP	URA3	(5)
pYM17	6HA *NatNT2*	NATNT2	(6)
pYM20	9myc *HphNT1*	HPHNT1	(6)
pRS316[GFP-ATG8]	ATG8prom::*GFP*::*ATG8*	URA3	(7)
p415		LEU2	(8)
pJS11	*BCY1* in pRS415	LEU2	(9)
pJS11-K313Q	*BCY1*-313Lys→Gln in pRS415	LEU2	This study
pJS11-K313,321Q	*BCY1*-313Lys→Gln-321Lys→Gln in pRS415	LEU2	This study
pJS11-K313R	*BCY1*-313Lys→Arg in pRS415	LEU2	This study
pJS11-K313,321R	*BCY1*-313Lys→Arg-321Lys→Arg in pRS415	LEU2	This study
pJS11-K88Q	*BCY1*-88Lys→Gln in pRS415	LEU2	This study
pJS11-K102Q	*BCY1*-102Lys→Gln in pRS415	LEU2	This study
pJS11-K88R	*BCY1*-88Lys→Arg in pRS415	LEU2	This study
pJS11-K102R	*BCY1*-102Lys→Arg in pRS415	LEU2	This study
pJS11-K321Q	*BCY1*-321Lys→Gln in pRS415	LEU2	This study
pJS11-K351Q	*BCY1*-351Lys→Gln in pRS415	LEU2	This study
pJS11-K321R	*BCY1*-321Lys→Arg in pRS415	LEU2	This study
pJS11-K351R	*BCY1*-351Lys→Arg in pRS415	LEU2	This study
pJS11-KmQ	*BCY1*-88Lys→Gln-102Lys→Gln-313Lys→Gln-321Lys→Gln-351Lys→Gln in pRS415	LEU2	This study
pYCJ1	*bcy1Cl* in pRS415	LEU2	(9)
pYCJ2	*bcy1ClI* in pRS415	LEU2	(9)
pCDNA-HA-Tip60 WT	*Tip60* in pCDNA-HA		(10)
pCI-flag PCAF	*PCAF* in pCI-flag		(11)

1. Sikorski RS, Hieter P (1989) A system of shuttle vectors and yeast host strains designed for efficient manipulation of DNA in *Saccharomyces cerevisiae*. *Genetics* 122(1):19–27.
2. Ramachandran V, Herman PK (2011) Antagonistic interactions between the cAMP-dependent protein kinase and Tor signaling pathways modulate cell growth in *Saccharomyces cerevisiae*. *Genetics* 187(2):441–454.
3. Leducq JB, et al. (2012) Evidence for the robustness of protein complexes to inter-species hybridization. *PLoS Genet* 8(12):e1003161.
4. Tarassov K, et al. (2008) An in vivo map of the yeast protein interactome. *Science* 320(5882):1465–1470.
5. Güldener U, Heck S, Fielder T, Beinhauer J, Hegemann JH (1996) A new efficient gene disruption cassette for repeated use in budding yeast. *Nucleic Acids Res* 24(13):2519–2524.
6. Janke C, et al. (2004) A versatile toolbox for PCR-based tagging of yeast genes: New fluorescent proteins, more markers and promoter substitution cassettes. *Yeast* 21(11):947–962.
7. Suzuki K, et al. (2001) The pre-autophagosomal structure organized by concerted functions of APG genes is essential for autophagosome formation. *EMBO J* 20(21):5971–5981.
8. Mumberg D, Müller R, Funk M (1995) Yeast vectors for the controlled expression of heterologous proteins in different genetic backgrounds. *Gene* 156(1):119–122.
9. Searle JS, Wood MD, Kaur M, Tobin DV, Sanchez Y (2011) Proteins in the nutrient-sensing and DNA damage checkpoint pathways cooperate to restrain mitotic progression following DNA damage. *PLoS Genet* 7(7):e1002176.
10. Legube G, et al. (2002) Tip60 is targeted to proteasome-mediated degradation by Mdm2 and accumulates after UV irradiation. *EMBO J* 21(7):1704–1712.
11. Yang XJ, Ogryzko VV, Nishikawa J, Howard BH, Nakatani Y (1996) A p300/CBP-associated factor that competes with the adenoviral oncoprotein E1A. *Nature* 382(6589):319–324.

Table S3. Culture media used in this study

Medium	Composition
YPD	1% yeast extract, 2% tryptone, 2% glucose, 2% agar
SC	0.17% yeast nitrogen base w/o amino acids, 2% glucose, amino acids drop-out, 2% agar
SC/MSG	0.17% yeast nitrogen base w/o amino acids and w/o ammonium sulfate, 0.1% monosodium glutamate, 2% glucose, amino acids drop-out, 2% agar
sel2n1.1	YPD + G418 + nourseothricin
sel2n1.2	YPD + G418 + HygB
spo1	1% potassium acetate, 0.1% yeast extract, 0.05% glucose, 12.5 mg/L uracil, 12.5 mg/L histidine, 12.5 mg/L leucine, 62.5 mg/L leucine, 2% agar, G418 (50 mg/L), nourseothricin (25 mg/L)
spo2	1% potassium acetate, 0.1% yeast extract, 0.05% glucose, 12.5 mg/L uracil, 12.5 mg/L histidine, 12.5 mg/L leucine, 62.5 mg/L leucine, 2% agar, G418 (50 mg/L), HygB (62.5 mg/L)
h1a	SC −His −Arg −Lys + Can + Lyp
h1α	SC −Leu −Arg −Lys + Can + Lyp
h3a	SC/MSG −His −Arg −Lys + Can + Lyp + G418
h3α	SC/MSG −Leu −Arg −Lys + Can + Lyp + G418
h5a	YPD + Can + Lyp + G418 + nourseothricin
h5α	YPD + Can + Lyp + G418 + HygB
sel2n2	YPD + G418 + nourseothricin + HygB
MTX/Glu	0.67% yeast nitrogen base w/o amino acids and w/o ammonium sulfate, 2% glucose, 2.5% noble agar, −Ade −Met −Lys drop-out (containing MSG), methotrexate
MTX/Gal	0.67% yeast nitrogen base w/o amino acids and w/o ammonium sulfate, 2% galactose, 2.5% noble agar, −Ade −Met −Lys drop-out (containing MSG), methotrexate
DMSO/Glu	0.67% yeast nitrogen base w/o amino acids and w/o ammonium sulfate, 2% glucose, 2.5% noble agar, −Ade −Met −Lys drop-out (containing MSG), 2% vol/vol DMSO
sel2nPCA	YPD + nourseothricin + HygB
5-FOA	0.17% yeast nitrogen base w/o amino acids and w/o ammonium sulfate, 2% glucose, amino acids drop-out, 1 g/L 5-fluoroorotic acid, 50 mg/L uracil, 2% agar
SC/PCA	0.67% yeast nitrogen base w/o amino acids and w/o ammonium sulfate, 2% glucose, amino acids drop-out (containing MSG), 2% agar

Can, canavanine; Lyp, thialysine.

Table S4. Antibiotic concentrations used in this study

Antibiotic	Final concentration, mg/L
G418	200
Nourseothricin	100
HygB	250
Can	50
Lyp	100
Methotrexate	200

Dataset S1. Compilation of PKA assay results with physical interaction evidence

Dataset S1

Dataset S2. Kinase–substrate pairs involving PKA subunits

Dataset S2

Dataset S3. MS experiments

Dataset S3

Dataset S4. MS experiments

Dataset S4

Dataset S5. Detailed GO enrichment analysis for each subset list

Dataset S5

Dataset S6. Protein complex analysis

Dataset S6

Interquartile mean and *P* values of each protein complex computed with COMPLEAT are reported for each PKA assay.

Dataset S7. Protein interactions tested by DHFR-PCA with and without methionine and rapamycin

Dataset S7

Dataset S8. Description of strains used in this study

Dataset S8

Dataset S9. Oligonucleotides used in this study

Dataset S9